



ORAL SURGERY

ORAL MEDICINE

ORAL PATHOLOGY

ORAL AND MAXILLOFACIAL PATHOLOGY

Editor: Carl M. Allen

Amelogenesis imperfecta and nephrocalcinosis syndrome

Case studies of clinical features and ultrastructure of tooth enamel in two siblings

R. K. Hall, MDS, FRACDS, FICD,^a P. Phakey, MSc, PhD, FAIP,^b
J. Palamara, Dip Ed, PhD, FAIP,^c and D. A. McCredie, MD, FRACP,^d
Melbourne, Australia

DEPARTMENT OF DENTISTRY, ROYAL CHILDREN'S HOSPITAL, DEPARTMENT OF PHYSICS,
MONASH UNIVERSITY, AND VICTORIAN RENAL SERVICE, ROYAL CHILDREN'S/ROYAL
MELBOURNE HOSPITALS

This article describes the enamel ultrastructure and clinical features in two siblings with the little known syndrome of Amelogenesis imperfecta and nephrocalcinosis. Nephrocalcinosis was diagnosed by x-ray examination of the abdomen, intravenous pyelography, ultrasonography, and computed tomography scan. Amelogenesis imperfecta was diagnosed from clinical and histologic examinations. The affected enamel was hypoplastic (~0.2 mm thick), positively birefringent, generally aprismatic, porous, and consisted of loosely packed, randomly orientated, thin (~10 nm wide), ribbonlike crystals. The enamel surface was rough, extensively cracked, and covered with ovoid or globular protrusions. Observations showed that in this case hypoplasia, hypocalcification, or hypomaturational defects were present in the same tooth, indicating that both secretory and maturation phases may have been affected. The study suggested the possibility of an abnormality in interstitial matrix, which could lead to dystrophic calcification in the kidney and abnormal tooth enamel formation. It also suggested the possibility of involvement of two separate but closely linked genes. (ORAL SURG ORAL MED ORAL PATHOL ORAL RADIOLOG ENDOD 1995;79:583-92)

Amelogenesis imperfecta (AI) is an incompletely understood group of hereditary developmental defects of dental hard tissues. Abnormal (or imperfect) tooth enamel occurs in all teeth of both primary and permanent dentitions, and this defect has no chronological developmental pattern and no recognized local or medical cause. AI occurs with a frequency of 1:700¹ to 1:14000² as an isolated defect. Inheritance is mainly autosomal dominant but autosomal recessive or x-linked inheritance can also occur.

Table I. Syndromes with Amelogenesis imperfecta as integral and diagnostic feature

Amelo-onycho-hypohidrotic syndrome
Morquio syndrome
Kohlschütter syndrome (Amelogenesis imperfecta, progressive neurologic deterioration, and epilepsy)
Amelogenesis imperfecta and nephrocalcinosis syndrome
Tricho-dento-osseous syndrome
Amelogenesis imperfecta with taurodontism
Oculo-dento-osseous dysplasia
Epidermolysis bullosa hereditaria

In addition a large number of syndromes may have non-AI-type developmental enamel defects as an associated feature.

Wide variation occurs in phenotype because of variable gene expression or different gene defects.³

AI also occurs as an integral and often diagnostic feature of a small number of syndromes (Table I). The inherited developmental enamel AI defects in

^aDirector & Chief Paediatric Dental Surgeon, Department of Dentistry, Royal Children's Hospital, Melbourne.

^bReader Department of Physics, Monash University, Melbourne; Hon. Research Fellow, Department of Dentistry, Royal Children's Hospital, Melbourne.

^cResearch Fellow, Department of Physics, Monash University, Melbourne.

^dNephrologist, Victorian Renal Service, Royal Children's/Royal Melbourne Hospitals, Melbourne.

Copyright © 1995 by Mosby-Year Book, Inc.
0030-4220/95/\$3.00 + 0 7/14/60618

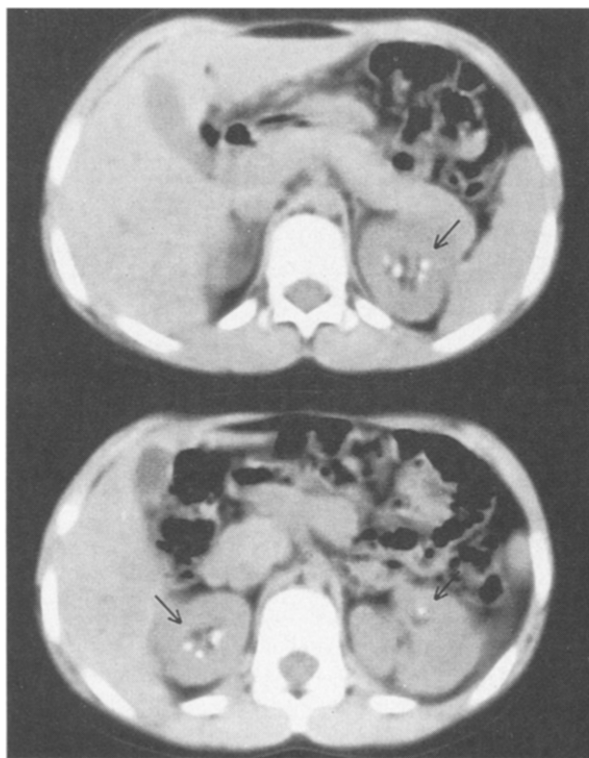


Fig. 1. Computed tomography scan showing nephrocalcinosis in both kidneys within tips of medullary pyramids and punctate calcification bilaterally in pelvis lying adjacent to internal iliac vessels.

these syndromes should be distinguished from the non-AI-type of developmental enamel defects variably found as an associated or possibly incidental feature in a large number of other syndromes and medical conditions. This article is a report of the enamel surface and ultrastructure of the teeth and of the clinical features in two siblings with the little known syndrome of Nephrocalcinosis and amelogenesis imperfecta. Nephrocalcinosis, which is the precipitation of calcium salts in renal tissue, is most commonly found in conditions associated with hypercalcemia or hypercalciuria such as renal tubular acidosis, Bartter's syndrome, medullary sponge kidney, and in hyperoxaluria. It is being reported with increased frequency as a result of drug-induced hypercalciuria whether from diuretics, steroid therapy, or vitamin D.⁴

CASE REPORTS

Case 1

A girl of Macedonian parents originally presented at the age of 10 years, 6 months with fever, rigors, and tenderness over the kidneys. A diagnosis of acute pyelonephritis was made, and she was treated with antibiotics. She had an uneventful but slow recovery. Examination revealed no other



Fig. 2. Clinical view of dentition of case 2 (age 14 years) showing abnormal worn and malformed primary and permanent tooth crowns and also gingival overgrowth caused by pathologic follicular remnants (in appearance almost identical to that of his sister).

abnormalities, apart from her dentition, and general development was normal. Her height was in the 10th percentile, and her weight was in the 30th percentile on the standard growth chart.

Investigation revealed no vesico-ureteric reflux on micraturating cysto-urethrogram, but nephrocalcinosis was found on the x-ray film of the abdomen and was confirmed by intravenous pyelography and computed tomography scan (Fig. 1). In addition bilateral pelvic calcification was found adjacent to the internal iliac vessels. It was thought to be probably in parailiac lymph glands. Blood electrolytes, urea, and creatinine levels were all normal.

Extensive investigation of calcium metabolism revealed no abnormality, and urine calcium, oxalate, and cystine were all normal. Serum vitamin D, parathyroid hormone (PTH), and osteocalcin levels were normal. Renal biopsy showed focal clusters of sclerosed glomeruli, although most glomeruli appeared normal. The predominant feature was infiltration of the interstitium with lymphocytes and plasma cells with marked periglomerular fibrosis. No calcification was seen in the biopsy sections.

Subsequent development has been normal, and the patient, who is now 15 years old, has no evidence of deteriorating renal function and has normal serum electrolytes, 3.0 mmol/L blood urea (reference range 2.1 mmol/L to 6.5 mmol/L >4 years of age), and 0.06 mmol/L creatinine (reference range 0.05 mmol/L to 0.11 mmol/L >16 years of age). Both kidneys were growing normally and appeared normal in outline on ultrasonography, although nephrocalcinosis persists virtually unchanged. Height and weight after puberty were both at the 75th percentile.

Twelve months before she presented to the hospital, this girl had attended the Royal Dental Hospital for investigation of opalescent teeth. AI was diagnosed on histologic examination of an extracted left primary central incisor tooth. At that time her brother (case 2), who was not seen, was reported to have teeth of similar appearance.

On examination at the Royal Children's Hospital many

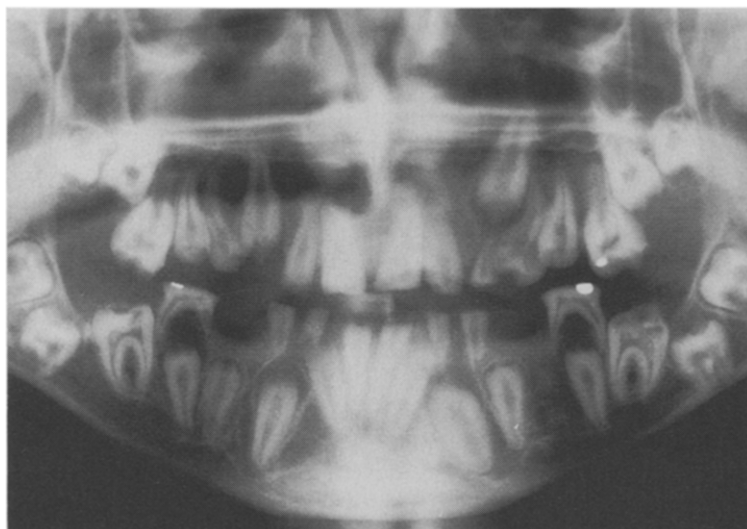


Fig. 3. Panoramic radiograph of case 2 (age 14 years) showing multiple unerupted permanent teeth devoid of normal enamel structure with reduced enamel thickness and lack of normal density. Impaction of developing permanent molars also shown. Intrapulpal calcification is seen in distal coronal pulp chambers of both lower first permanent molar teeth. (Reprinted with permission from Hall RK. *Pediatric orofacial medicine and pathology*. London: Chapman & Hall, 1994.)

retained, worn-down, yellow/brown primary teeth with thin or absent enamel were seen. The condition was confirmed on clinical examination as AI, which was thought to be of autosomal recessive Witkop Type 1G (enamel agenesis type).³ Gingival overgrowth and an anterior open bite were also noted. Panoramic and cephalometric radiographs were taken before the retained primary teeth were removed. Surgical exposure and composite resin bonding of the enamel-deficient crowns of the permanent central incisors were done to protect them from wear. These teeth, however, subsequently developed pulp necrosis that required endodontic treatment.

A more radical approach was subsequently decided on in view of the outcome of the other reported cases, and all unerupted incisors were removed. Alveolectomy and soft-tissue reduction were done. These procedures allowed construction of dentures to give the most satisfactory aesthetic result possible and to thus improve self-esteem.

Case 2

The elder brother of case 1 was first seen at the Royal Children's Hospital. He was 14 years, 8 months. He was seen after nephrocalcinosis was diagnosed in his sister (case 1). He was a normal healthy boy, and apart from malformed teeth, no abnormalities were found on examination. His height was in the 10th percentile, and his weight was in the 25th percentile. Ultrasonography showed nephrocalcinosis in both kidneys. Investigations showed no disturbance in calcium metabolism or excretion, and renal function was normal. Serum Vitamin D, PTH, and osteocalcin levels were all normal. Renal biopsy showed a mild degree of interstitial infiltration with inflammatory cells. This infiltration was similar to that of case 1, although much milder. Again no calcification was evident on biopsy. Serum urea

and electrolytes were normal, although creatinine level was at the upper limit of normal (120 $\mu\text{mol/L}$).

Subsequent development has also been normal, although changes of nephrocalcinosis persist on ultrasonography. At 19 years of age the patient is very healthy, and both his height and weight are in the 75th percentile. This boy, like his sister, had been noted to have abnormal teeth. Dental examination at the Royal Children's Hospital showed retained, yellow, primary teeth and severely worn permanent teeth (incisors and second molars) with virtually no enamel visible. The only permanent teeth erupted were the maxillary incisors, first molars, and the two left premolars. The patient clearly had AI of the same type as his sister. He had gingival overgrowth especially associated with the hypoplastic incisors but had no anterior open bite (Fig. 2). A panoramic radiograph (Fig. 3) showed coronal intrapulpal calcifications present in both dysplastic lower first permanent molars.

No family history was reported of either amelogenesis imperfecta or renal problems, and no known consanguinity was present. Dental management, as for that of his sister (case 1), involved removal of all nonviable permanent teeth and the construction of dentures. A third middle female sibling was healthy and had no dental or renal abnormalities.

ULTRASTRUCTURAL STUDIES OF AFFECTED TOOTH ENAMEL

Few transmission electron microscopic ultrastructural studies⁵⁻⁷ of AI have been done because of the difficulties of preparing ultrathin samples of tissues. However, the technique of selected-area argon-ion-beam-thinning⁸ has been successful in preparation of

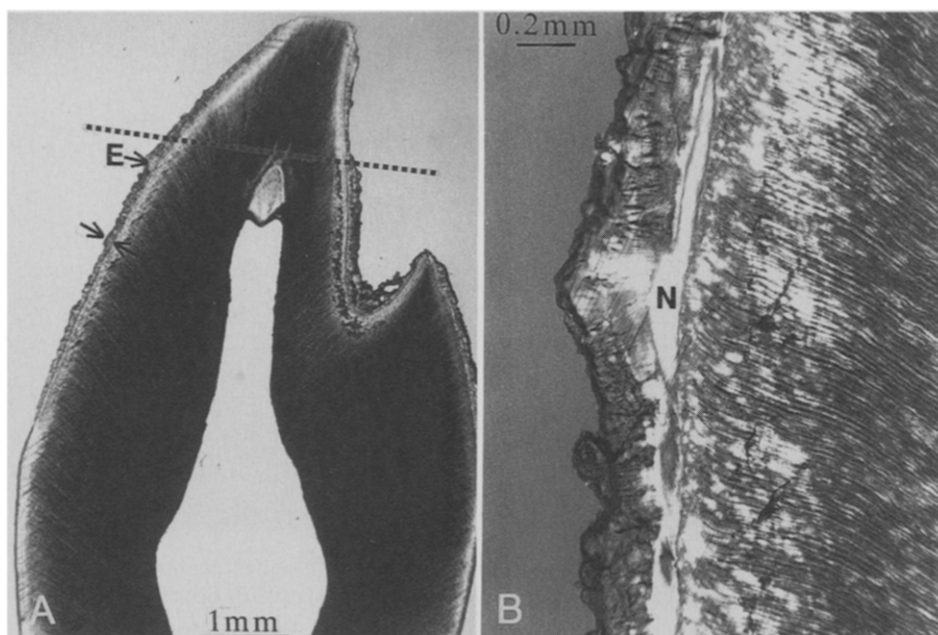


Fig. 4. Transmitted light micrographs of thin section of partially erupted tooth after imbibition in water. **A**, low magnification showing enamel (between arrows) is much thinner (~ 0.2 mm) than normal healthy enamel (~ 1.0 to 2.5 mm) (dotted line marks boundary between erupted and unerupted enamel). Some enamel has been lost from erupted enamel near incisal edge. **B**, Crossed polarized light micrograph of area *E* in **A** shows that enamel is positively birefringent, but some negatively birefringent areas (*N*) are present near the dentino-enamel junction. (Reprinted with permission from Hall RK. Pediatric orofacial medicine and pathology. London: Chapman & Hall, 1994.)

ultrathin samples and in elucidation of the ultrastructure of healthy enamel,^{9, 10} early enamel caries,¹¹⁻¹³ surface enamel,^{14, 15} and a particular type of AI that causes pigmented enamel in Polynesian teeth.¹⁶ One of the permanent incisors (tooth 12) from case 1, which had only the incisal edge erupted through the mucosa was submitted for histologic and ultrastructural investigation of the enamel structure with light microscopy, scanning electron microscopy, and transmission electron microscopy.

METHODS

For light microscope (LM) observations with transmitted light, longitudinal sections of the tooth were cut with a slow-speed diamond saw. Each section was handlapped to a thickness of ~ 80 μ m, polished on both sides, and then examined in air and water with a LM. Measurements of the enamel thickness relative to the dentine and also relative to normal healthy enamel were made from the LM observations with a graduated graticule. The sign of the birefringence of the enamel was determined from the lapped and polished thin sections after the sections were imbibed with water and examined in a polarized LM with crossed polarizers.

The surface topography of the erupted and unerupted enamel of the tooth was investigated with a Hitachi S/570 (Hitachi Ltd, Tokyo, Japan) scanning electron microscope operating at accelerating potentials of 20 and 30 KV. Intact surfaces of enamel were examined; they were not etched but were coated with a thin conducting layer of platinum before examination. Ultrastructural investigation of selected areas of enamel and dentine were made with a transmission electron microscope (TEM). For this procedure ultrathin sections were prepared by selected area argon-ion-beam-thinning technique as developed by Phahey et al.⁸ Areas of interest in the thin sections were selected with a LM and enclosed by cementing a slotted grid on the sample. The mounted sample was then placed in an argon-ion-beam-thinning unit and was thinned from both sides by argon-ions at a glancing angle of 15° , until a small perforation appeared in the previously selected area in the sample. The areas immediately surrounding the perforation were suitable for TEM observations. All TEM samples were coated with a thin layer of carbon before they were examined in a JEOL 200CX (JEOL Ltd, Tokyo, Japan), electron microscope operating at 200 KV. Selected area electron diffraction was used in the

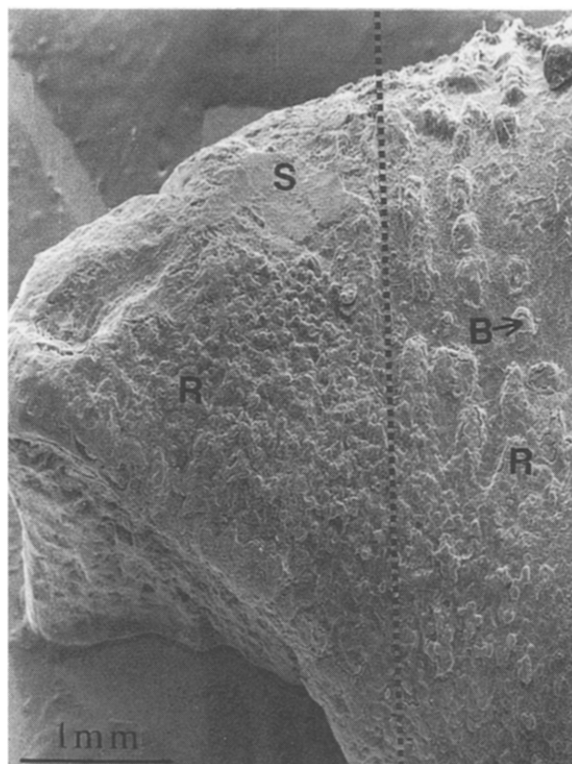


Fig. 5. Scanning electron micrograph of surface of tooth showing erupted enamel on left and unerupted enamel on right of dotted line. Unerupted enamel surface shows ovoid or globular protrusions (*B*) and rough enamel (*R*). Erupted enamel surface shows rough enamel (*R*) and smooth-looking, apparently worn enamel (*S*).

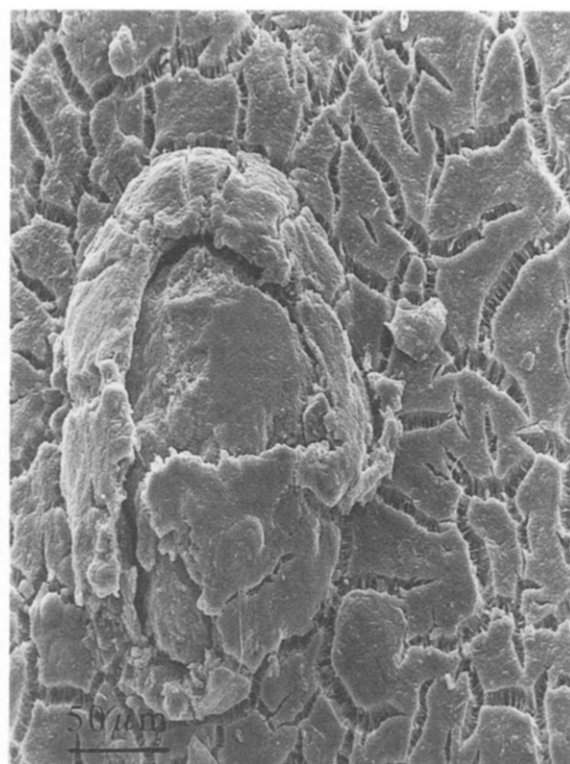


Fig. 6. Scanning electron micrograph of ovoid protrusion (*B*) in Fig. 5. Extensive cracks are present in unerupted enamel surface. Partial occlusion of cracks by threadlike material bridging their sides can also be seen. (Reprinted with permission from Hall RK. Pediatric orofacial medicine and pathology. London: Chapman & Hall, 1994.)

identification of the crystal structure and in the assessment of the crystal orientation.

ULTRASTRUCTURAL OBSERVATIONS

LM observations showed that the affected tooth (case 1) had a very thin layer of enamel that was nearly nonexistent in some areas. The maximum enamel thickness was ~ 0.2 mm, which is much thinner than that of comparable normal healthy enamel (1.0 to 2.5 mm)¹⁷ (Fig. 4, *A*). The enamel surface was very irregular. By polarized light microscopy of thin sections imbibed in air or water, it was found that unlike the healthy enamel the birefringence of enamel in the sections examined was positive (Fig. 4, *B*). A few pockets of negatively birefringent enamel were present close to the dentine-enamel junction.

Surface topography of the unerupted portion of enamel examined by scanning electron microscopy showed that some areas were rough but that others were mostly covered with ovoid or globular protrusions ("tubercles") (Figs. 5 and 6). Extensive cracks

occluded with a threadlike material that appeared to bridge the sides of the cracks were present in all areas of the unerupted enamel (Figs. 6 and 7). The surface of the erupted portion of enamel showed rough enamel and smooth-looking areas (Fig. 5) that were apparently caused by wear. In the smooth-looking areas the ovoid or globular protrusions were absent, and the cracks were wider than those in unerupted enamel and were free of any occluding material (Fig. 8).

The ultrastructure of both erupted and unerupted affected enamel was similar as revealed by transmission electron microscopy. This enamel consisted of loosely packed, randomly oriented, thin, ribbonlike crystals that were ~ 10 nm wide (Figs. 9 and 10). The well-defined prismatic structure seen in normal healthy enamel (Fig. 11) was absent or very poorly developed (Fig. 10). The poor packing of the ribbonlike enamel crystals caused porosity in the affected enamel. Whether the pores were empty or had an organic or amorphous content could not be determined from the TEM observations or the selected area elec-

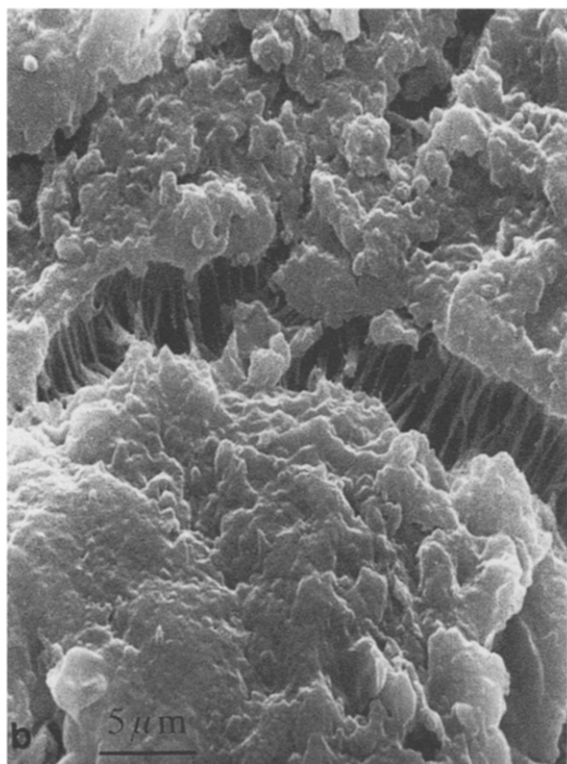


Fig. 7. Scanning electron micrographs of rough unerupted enamel in Fig. 5 showing threadlike material bridging cracks seen in Fig. 5.

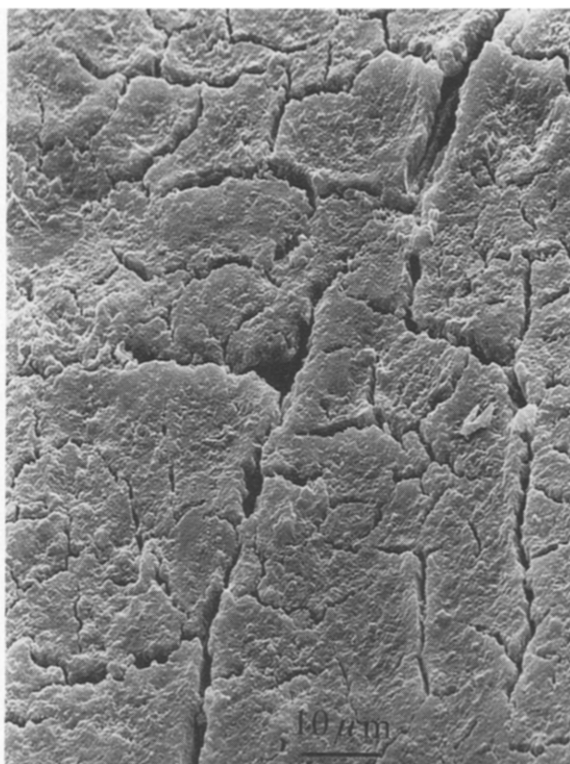


Fig. 8. Higher magnification scanning electron micrograph of apparently worn surface (area S in Fig. 5) in erupted enamel showing extensive cracks in surface and absence of occluding material in cracks (compare with Figs. 6 and 7).

tron diffraction patterns, which identified the presence of only an hydroxyapatite phase. The width of the ribbonlike crystals compared well with those of dentine crystals near the dentine-enamel junction in the sample and in the normal healthy tooth. Although the loosely packed ribbonlike crystals ~ 10 nm wide were common in most areas of affected enamel, occasional closely packed ribbonlike crystals of smaller width (~ 5 nm) were present in some areas.

DISCUSSION

AI has been classified by Witkop³ and Witkop and Sauk¹⁸ on the basis of hereditary and pathologic type and by Sundell and Koch¹⁹ on clinical and pathologic appearance. Three main pathologic types of amelogenesis imperfecta, namely hypoplastic, hypocalcified, and hypomaturational types,³ are currently recognized.

AI hypoplasia-type covers a spectrum of abnormalities of enamel form in which a primary organic matrix defect appears to exist. Variable reduction is seen in thickness of enamel (often 60%). The enamel is either thin, smooth, and pitted or is rough with pits and craters. Other hypoplastic types show severe pit-

ting and areas of hypomineralization.⁷ Communication with the dentino-enamel junction frequently occurs. In AI Hypocalcified type there is initial deposition of smaller than normal, poorly packed crystals with resultant macroporosities and fibrillar disoriented surface prisms with hypocalcification of prism sheaths and surface. The enamel is yellow-brown.²⁰ In AI hypomaturational type there is altered maturation of enamel-matrix caused by changes in the protein after initial deposition and mineralization. During normal amelogenesis the amino-acid profile alters from that of mainly proline, leucine, and histidine in initially deposited matrix to that of mainly aspartic acid and alanine in mature enamel. Disturbance of the normal maturation process results in retention of organic protein material within the enamel, smaller enamel crystallites, and abnormal prism structure.^{21, 22} In many cases, however, no clear-cut distinction between types is possible,²³⁻²⁵ and it can be demonstrated at the ultrastructural level, as in this case, that both hypoplastic and hypomaturational defects occur in the same tooth. Therefore the present

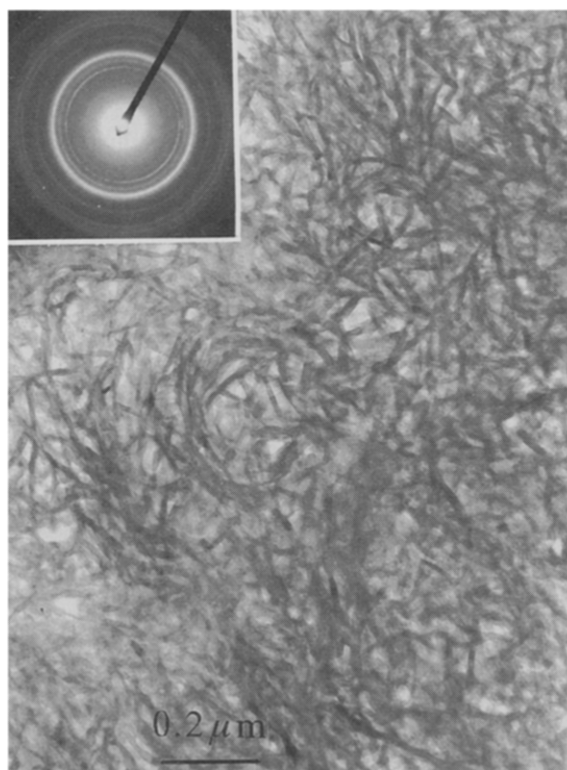


Fig. 9. Transmission electron micrograph showing loosely packed and randomly oriented ribbonlike enamel crystals in unerupted enamel. *Inset*, selected area electron diffraction pattern of crystals showing diffuse but continuous diffraction rings confirming small size and random orientation of crystals.

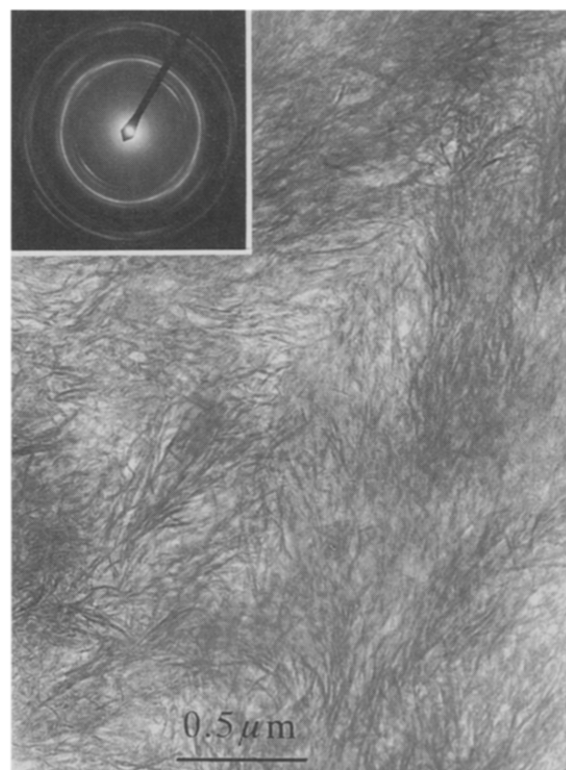


Fig. 10. Transmission electron micrograph showing fine ribbonlike enamel crystals in pseudoprismatic arrangement. *Inset*, selected area electron diffraction pattern showing diffuse and discontinuous diffraction rings indicating that crystals are small and have some preferred orientation. (Reprinted with permission from Hall RK. Pediatric orofacial medicine and pathology. London: Chapman & Hall, 1994.)

classification may not appropriately categorize the different patterns of inheritance and phenotypic expressions of this group of conditions.

Amelogenins are the first enamel proteins secreted, they have a molecular weight of approximately 25,000 d and are derived from a single gene. The proteins in mature enamel (called enamelines or nonamelogenins) are retained degradation products of amelogenin. They have a higher molecular weight (50,000 to 70,000 d) and are bound to mineral.²⁶

The amelogenin gene has now been precisely mapped in both mouse and man.²⁷⁻²⁹ The human genome contains two copies of the amelogenin gene: one on the X chromosome at p22.1 to 22.3 on the distal short arm and one in the pericentromeric region on the Y chromosome. X-linked amelogenesis imperfecta has been mapped by linkage to the same region,³⁰ making it likely that in X-linked amelogenesis imperfecta, at least, it is the synthesis of the amelogenin group of enamel proteins that is abnormal.

It has been recognized for some time that AI occurs

as an integral feature of certain syndromes³¹⁻³³ (Table I). The difficulty of differentiating between AI as an isolated entity and the identical dental phenotypic feature as one component of a syndrome has been well presented in relation to Tricho-dento-osseous syndrome and type IV hypomaturation-hypoplastic with taurodontism (H-H-T) amelogenesis imperfecta^{34, 35}; the other phenotypic features of hair and bone changes had sometimes been overlooked by dentists in reported cases of AI, and TDO syndrome had therefore not been recognized.

Our patients showed no evidence of abnormality in calcium metabolism or excretion, and oxalate excretion was also normal. Renal biopsy of the cortex showed no evidence of calcium deposition, which suggested that the calcification was confined to renal medulla. However, interstitial cellular infiltration was present in the biopsies of both patients, and nephrocalcinosis has been described in association with

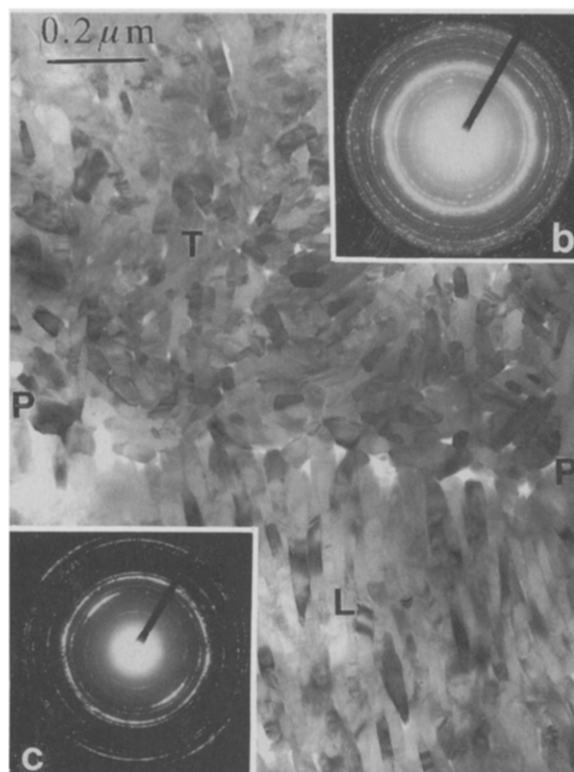


Fig. 11. Transmission electron micrograph of normal enamel for comparison with Figs. 9 and 10 showing well-packed enamel crystals seen in nearly longitudinal orientation in area *L* and in transverse orientation in area *T* on other side of prism boundary *PP*. Insets (*b* and *c*), selected area electron diffraction patterns show sharp spots in diffraction rings as compared with insets of Figs. 9 and 10. Lower selected area electron diffraction pattern shows preferred orientation of longitudinal crystals *L* indicated by discontinuous rings as compared with upper selected area electron diffraction pattern, which is from area *T* of transverse crystals. (Reprinted with permission from Hall RK. Pediatric orofacial medicine and pathology. London: Chapman & Hall, 1994.)

interstitial nephritis.³⁶ This infiltration could suggest the possibility of an abnormality in interstitial matrix, which may lead to dystrophic calcification in the kidney and abnormal enamel production in the tooth. Alternatively two separate but closely linked genes could be involved.

In 1985 Lubinsky et al.³⁷ described a syndrome of Amelogenesis imperfecta, nephrocalcinosis, impaired renal concentration, and possible abnormality of calcium metabolism in two siblings. They reported raised osteocalcin levels, but these levels were normal in our patients. Their paper cited an earlier paper by MacGibbon³⁸ in which AI and nephrocalcinosis were reported in a young woman (these had been recognized

from the time the patient was 11 years of age) when her 26-year-old brother with nephrocalcinosis and similar teeth died.

In the cases described here the affected enamel of all primary and permanent teeth was thin, and the erupted surfaces, although clinically smooth because of wear, were microscopically rough, and the unerupted areas of enamel indicated that the affected enamel was markedly hypoplastic. When the hypoplasia, color, and anterior open bite present (case 1) were compared with Witkop's classification,³ it was considered that the most likely type of AI was Witkop Type 1G (enamel agenesis, autosomal recessive type).

Scanning electron microscopy observations reported here have shown that the surface topography of the affected enamel with its cracks and ovoid or globular protrusions was very different from that of normal healthy enamel¹⁴ and other reported hypoplastic teeth.^{7, 20, 22} The polarized light observation that the affected enamel was positively birefringent and hence porous agreed well with the ultrastructural findings with the TEM. No quantitative estimates of porosity could be made, because it was not possible to find from the electron diffraction data whether the pores were empty or had an organic content. TEM observations suggested that the pockets of enamel with negative birefringence observed with the LM could perhaps be due to the close packing of small (~5 nm) ribbonlike enamel crystals present in these pockets.

The absence of the ovoid or globular protrusions in the relatively small area of erupted enamel indicated that the affected enamel wears rapidly after eruption. The enlargement of the cracks and the loss of the occluding material in the erupted enamel caused by wear pointed to the detrimental role of the cracks in providing pathways into the enamel.

The ultrastructure of the affected enamel revealed by transmission electron microscopy was very different from that of normal healthy enamel (Fig. 11), the more common type of hypoplastic enamel, and the Polynesian pigmented tooth enamel.^{22, 16} The main differences were increased porosity, ribbonlike enamel crystals (width ~10 nm), random and loose packing of crystals, the lack of prisms, and an appearance similar to that of coronal cementum of an acellular and afibrillar type found in other species. A similar appearance was described by Ooya et al.³⁹ in the calcified tissues above the hypoplastic enamel surface in autosomal recessive rough hypoplastic AI. The size of the ribbonlike crystals (~10 nm) was similar to that of the earliest formed enamel crystals. It appeared that once the initially nucleated crystals became rib-

bonlike, the growth was hindered, and the crystals failed to achieve the size and packing of mature enamel crystals. Hypomaturation type defects are currently thought to be due to an inhibition of proteolysis, which results in decreased protein removal and hence protein retention in and around enamel prisms. Protein retention would interfere with crystallite growth and prism delineation. The inhibition of proteolysis is caused by a chemical or structural aberration in the protein, by an enzyme defect in the maturation pathway, or by reduced quantities or activity of protease necessary for amelogenin degradation. The presence of crystals of smaller width (~5 nm) than that of the ribbonlike crystals indicated that some degree of hypocalcification may also be present.

It was quite evident from the clinical and ultrastructural studies reported here that in this case, as in other types of AI (with the exception perhaps of the X-linked type), hypoplasia together with hypocalcification or hypomaturation defects were present together in the same tooth, thus indicating that both the secretory and maturation phases may be commonly affected in AI.

CONCLUSION

The ultrastructure of the affected enamel revealed by our investigations strongly points to a genetic disorder or other factors causing hypocalcification and hypomaturation of the enamel crystals and hypoplasia of the enamel matrix.

Other authors have found it impossible to distinguish between clinical phenotypes of AI with polarized light microscopy, scanning electron microscopy, or secondary ion mass spectroscopy.²⁵

Ultrastructural studies and estimation of protein content and amino-acid profile may become increasingly important diagnostic tools in differentiating types of AI because of variability of clinical presentation. This variability results from eruptive loss of pathologic enamel and posteruptive enamel loss caused by the environmental factors of wear and exposure to the oral environment. It also results from the frequent difficulty of obtaining an accurate pedigree, because of the increased trend toward family dispersal and movement from country to country.⁴⁰

Because few patients have been reported with this particular syndrome, the prognosis is unknown. In the cases reported by MacGibbon,³⁸ although renal function was stable until the patient was 16 years of age, progressive renal failure and death ensued. The recognition and study of other cases of amelogenesis imperfecta and nephrocalcinosis syndrome are therefore most important.

All children with AI and their parents should be

questioned regarding existing or past medical problems with particular reference to the urinary tract. Urine should be examined for presence of infection and proteinuria, and the child should be referred for medical examination including renal function studies and ultrasonography to detect nephrocalcinosis. Similarly, children with unexplained nephrocalcinosis should have careful specialist pediatric dentistry examination for dental developmental tooth enamel abnormalities, if the teeth appear at all unusual. The importance of syndrome diagnosis and recognition in this condition is in guiding dentists to recognize the possibility of the presence of other anomalies in patients with AI.

We acknowledge the help given by the Educational Resource Centre and the Department of Radiology, Royal Children's Hospital, Melbourne, for the clinical photographs, computed tomography, and ultrasonography images in Figs. 1-3, and the photographic unit of the Department of Physics, Monash University, for the photo micrographs in Figs. 7-11, and also Dr. Hector Orams, who reported on the original biopsy, for his critical review of the manuscript, and Dr. Anthony Dickinson, Prosthodontist, who has participated in the treatment of these children.

REFERENCES

1. Bäckman B, Holm A-K. Amelogenesis imperfecta: prevalence and incidence in a northern Swedish county. *Community Dent Oral Epidemiol* 1956;14:43-7.
2. Witkop CJ Jr. Hereditary defects in enamel and dentine. *Acta Genet Med Gemellol (Roma)* 1957;7:236-9.
3. Witkop CJ Jr. Amelogenesis imperfecta, dentinogenesis imperfecta, and dentine dysplasia revisited: problems in classification. *J Oral Pathol Med* 1989;17:547-53.
4. Schultz PK, Strife JL, Strife CF, McDaniel JD. Hyperechoic renal medullary pyramids in infants and children. *Pediatr Radiol* 1991;181:163-7.
5. Kerebel B, Daculsi G. Amelogenesis imperfecta—étude structurale, ultrastructurale et radiocristallographique. *J Biol Buccale* 1976;4:43-60.
6. Kerebel B, Daculsi G. Ultrastructural study of amelogenesis imperfecta. *Calcif Tissue Res* 1977;24:191-7.
7. Wright JT, Robinson C, Shore R. Characterization of the enamel ultrastructure and mineral content in hypoplastic amelogenesis imperfecta. *ORAL SURG ORAL MED ORAL PATHOL* 1991;72:594-601.
8. Phakey PP, Rachinger WA, Orams HJ, Carmichael GC. Preparation of thin sections of selected areas. In: Sanders JV, Goodchild DJ, eds. *Electron microscopy*. Vol 1. Canberra, Australia: Australian Academy of Science, 1974:412-3.
9. Orams HJ, Phakey PP, Rachinger WA, Zyberty J. Visualization of micropore structure in human dental enamel. *Nature* 1974;252:584-5.
10. Orams HJ, Zyberty JJ, Phakey PP, Rachinger WA. Ultrastructural studies of human dental enamel using selected-area argon-ion-beam thinning. *Arch Oral Biol* 1976;21:663-76.
11. Orams HJ, Phakey PP, Rachinger WA, Zyberty JJ. Ultrastructural changes in translucent and dark zones of early enamel caries. *J Oral Pathol Med* 1980;9:54-61.
12. Palamara J, Phakey PP, Rachinger WA, Orams HJ. Ultrastructure of the intact surface zone of white spot and brown spot carious lesions in human enamel. *J Oral Pathol Med* 1986;15:28-35.

13. Palamara J, Phakey PP, Rachinger WA, Orams HJ. Laminated zones in carious human dental enamel. *J Oral Pathol Med* 1986;15:109-14.
14. Palamara J, Phakey PP, Rachinger WA, Orams HJ. Electron microscopy of surface enamel of human unerupted and erupted teeth. *Arch Oral Biol* 1980;25:715-25.
15. Palamara J, Phakey PP, Rachinger WA, Orams HJ. The ultrastructure of spindles and tufts in human dental enamel. *Adv Dent Res* 1989;3:249-57.
16. Rodda JC, Palamara J, Phakey PP, Smillie AC. Polarized light microscopy and ultrastructure of Polynesian pigmented tooth enamel. *Arch Oral Biol* 1989;34:475-81.
17. Orban's oral histology and embryology. Bhaskar SN, ed. 11th ed. St. Louis: Mosby-Year Book, 1990:49.
18. Witkop CJ Jr, Sauk JJ Jr. Heritable defects of enamel. In: Stewart RE, Prescott GH, eds. *Oral facial genetics*. St. Louis: CV Mosby, 1976:151-226.
19. Sundell S, Koch G. Hereditary amelogenesis imperfecta: I. epidemiology and clinical classification in a Swedish child population. *Swed Dent J* 1985;9:157-69.
20. Sauk JJ Jr, Cotton WR, Lyon HW, Witkop CJ Jr. Electron-optic analyses of hypomineralized amelogenesis imperfecta in man. *Archs Oral Biol* 1972;17:771-9.
21. Wright JT, Butler WT. Alteration of enamel proteins in hypomaturation amelogenesis imperfecta. *J Dent Res* 1989;68:1328-30.
22. Wright JT, Lord V, Robinson C, Shore R. Enamel ultrastructure in pigmented hypomaturation amelogenesis imperfecta. *J Oral Pathol Med* 1992;21:390-4.
23. Bäckman B, Anneroth G. Microradiographic study of amelogenesis imperfecta. *Scand J Dent Res* 1989;97:316-29.
24. Bäckman B, Anneroth G, Hörstedt P. Amelogenesis imperfecta: a scanning electron microscopic and microradiographic study. *J Oral Pathol Med* 1989;18:140-5.
25. Bäckman B, Lundgren T, Engstrom EU, et al. The absence of correlations between a clinical classification and ultrastructural findings in amelogenesis imperfecta. *Acta Odontol Scand* 1993;51:79-89.
26. Termine JD, Belcourt AB, Christner PJ, Conn KM, Nysten MV. Properties of dissociatively extracted fetal tooth matrix proteins. I principal molecular species in developing bovine enamel. *J Biol Chem* 1980;255:9760-8.
27. Snead ML, Zeichner-David M, Chandra T, Robson KJH, Woo SLC, Slavkin HC. Construction and identification of mouse amelogenin with DNA clones. *Proc Natl Acad Sci USA* 1983;80:7254-8.
28. Snead ML, Lau EC, Fincham AG, Zeichner-David M, Davis C, Slavkin HC. Of mice and men: anatomy of the amelogenin gene. *Connect Tissue Res* 1989;22:101-9.
29. Lau EC, Slavkin HC, Snead ML. Analysis of human enamel genes: insights into genetic disorders of enamel. *Cleft Palate Craniofac J* 1990;27:121-30.
30. Lagerström M, Dahl N, Iselius L, Bäckman B, Pettersson V. Mapping the gene for x-linked amelogenesis imperfecta by linkage analysis. *Am J Hum Genet* 1990;46:120-5.
31. Gorlin R, Cohen MM Jr, Levin IS. *Syndromes of the head and neck*. New York: Oxford University Press, 1990:99-113, 234-5, 501-6, 861-6.
32. Christodoulou J, Hall RK, Menahem S, Hopkins JJ, Rogers J. A syndrome of epilepsy, dementia, and amelogenesis imperfecta: genetic and clinical features. *J Med Genet* 1988;25:827-30.
33. Hall RK. *Paediatric orofacial medicine and pathology*. London: Chapman and Hall, 1994:195-202.
34. Crawford PJM, Aldred MJ. Amelogenesis imperfecta with taurodontism and tricho-dento-osseous syndrome: Separate conditions or a spectrum of disease? *Clin Genet* 1990;38:44-50.
35. Quattromani FSD, Shapiro RS, Young RJ, et al. Clinical heterogeneity in the tricho-dento-osseous syndrome. *Hum Genet* 1983;64:116-21.
36. Kessel D, Hall CM, Shaw DG. Two unusual cases of nephrocalcinosis in infancy. *Pediatr Radiol* 1992;22:470-1.
37. Lubinsky M, Angle C, Waynemark P, Witkop CJ Jr. Syndrome of amelogenesis imperfecta nephrocalcinosis, impaired renal concentration, and possible abnormality of calcium metabolism. *Am J Med Genet* 1985;20:233-43.
38. MacGibbon D. Generalized enamel hypoplasia and renal dysfunction. *Aust Dent J* 1972;17:61-3.
39. Ooya K, Nalbandian J, Naikura T. Autosomal recessive rough hypoplastic amelogenesis imperfecta. *ORAL SURG ORAL MED ORAL PATHOL* 1988;65:449-58.
40. Wright JT, Robinson C, Kirkham J. Enamel protein in smooth hypoplastic amelogenesis imperfecta. *Pediatr Dent* 1992;14:331-7.

Reprint requests:

Roger K. Hall, MDSc, FRACDS, FICD
Department of Dentistry
Royal Children's Hospital
Flemington Rd.
Parkville, Victoria 3052